

Squeeze Flow Rheometer

Adeniyi Lawal and Dilhan M. Kalyon
Highly Filled Materials Institute
Stevens Institute of Technology
Castle Point, Hoboken, NJ 07030

Abstract

The squeeze flow rheometer is widely used especially for the rheological characterization of composites and polymer melts. However, since it incorporates both shear and extensional deformations its use is not straightforward. Here the two-dimensional constant-speed squeezing flow of viscoplastic fluids between two approaching surfaces in relative motion is solved using the Finite Element Method. Slip at the wall, a condition generally encountered with viscoplastic fluids at solid surfaces, is incorporated in the model. The analysis is applicable to the rheological characterization and testing of parameters of constitutive equations for filled polymers and elastomers that exhibit a yield stress and will expand our understanding of the squeeze flow rheometer. The numerical analysis was focused on the determination of conditions under which 1-D analysis is valid.

Introduction

The squeeze flow rheometer involves both shear and extensional deformations (1). Under carefully selected conditions it can be used as a rheometer to characterize the shear viscosity (2-6) and upon lubrication of rheometer surfaces, for characterization of biaxial extensional viscosity (7-8). Under relatively slow squeezing rates (low Deborah number) the elasticity of the fluid need not be considered and the generalized Newtonian fluid constitutive equation is sufficient to represent the squeeze flow behavior of polymer melts and suspensions (5, 9-11). For power law fluids, the use of the lubrication assumption is allowed for analysis of squeeze flow for limited ranges of squeeze rates and gap over radius (h/R) ratios (2,3,11,12). For viscoplastic fluids, the squeeze flow takes place under conditions where all of the fluid is yielded (13,14), unlike rectilinear viscometric flows which allow the formation of an undeformed plug (15). FEM based numerical solutions are available for viscoplastic fluids (16,17) and rely on the use of a bi-viscosity type shear viscosity material function which allows deformation, albeit under a large shear viscosity for stress magnitude values which are below the yield stress. The deformation of viscoplastic fluids is generally accompanied by wall slip (15,18) and none of the earlier simulation studies for the squeeze flow of viscoplastic fluids have incorporated wall slip during squeeze flow. In the

following, we provide 2-D Finite Element Method based numerical simulations of the squeezing flow of viscoplastic fluids subject to wall slip. Furthermore, comparisons with the recently available analytical solutions of squeezing flow of viscoplastic fluids with wall slip (18) are made.

Analysis

The viscoplastic fluid is contained in the gap formed by two horizontal parallel circular disks that are of the same radius R , and are both initially at rest. The fluid subsequently undergoes squeezing action by either applying a constant force F to the top disk or by moving it at a constant speed \dot{h} , with the bottom disk remaining at rest. If the applied force is constant, the speed of the top disk will vary with time, and vice-versa. The flow is dominated by viscous effects, thus permitting the treatment of the flow as quasi-static, i.e., the flow is steady at any instant of time, and the time derivatives of the equations of conservation of mass and momentum can be ignored. The inertia effect is negligible because of the highly viscous nature of materials of interest and the creeping nature of the resulting flow. The flow is axisymmetric, and if gravitational effects are neglected, the applicable equations of conservation of mass and momentum are given by:

$$\begin{aligned}0 &= \frac{1}{r} \frac{\partial r u_r}{\partial r} + \frac{\partial u_z}{\partial z} \\0 &= -\frac{\partial p}{\partial r} - \left(\frac{1}{r} \frac{\partial r \tau_{rr}}{\partial r} - \frac{\tau_{\theta\theta}}{r} + \frac{\partial \tau_{rz}}{\partial z} \right) \\0 &= -\frac{\partial p}{\partial z} - \left(\frac{1}{r} \frac{\partial r \tau_{rz}}{\partial r} + \frac{\partial \tau_{zz}}{\partial z} \right)\end{aligned}\tag{1-3}$$

where r and z are the radial and axial coordinates respectively, u_r and u_z the corresponding velocities, p is the pressure, τ_{rr} , $\tau_{\theta\theta}$ and τ_{zz} are the components of the stress tensor. The penalty/ Galerkin Finite Element Method is employed in the solution of Eqs. 2-3 using a large positive number λ_p (penalty parameter = 10^6):

$$p = -\lambda_p \eta \left(\frac{1}{r} \frac{\partial u_r}{\partial r} + \frac{\partial u_z}{\partial z} \right) \quad (4)$$

Boundary Conditions

On the line of symmetry, i.e., at $r=0$, the r -component of the equation of conservation of momentum is replaced by the condition,

$$u_r = 0 \quad (5)$$

while in the z -component equation,

$$\tau_{rz} = 0 \quad (6)$$

At the fluid/air interface, i.e., at $r=R$

$$p + \tau_{rr} = 0, \quad \tau_{rz} = 0 \quad (7)$$

where the air is assumed to exert no tangential or normal viscous stress on the interface and the ambient pressure exerted by the air at the edge of the disks, i.e., at $R=1$ has been set to zero for convenience. At the fluid/solid interfaces at the upper and lower disks, the z -component of the equation of conservation of momentum is replaced by the kinematic condition which implies that:

$$u_z(z=h) = \dot{h} \quad \text{and} \quad u_z(z=0) = 0 \quad (8)$$

while the Navier's wall slip boundary condition is applied to the tangential or r -component of the equation of momentum. The condition of wall slip can be expressed as

$$\underline{t} \cdot (\underline{u} - \underline{u}_{\text{solid}}) = \beta (\underline{t} \underline{t} : \underline{T}) \quad (9)$$

where \underline{t} is the unit tangent vector to the surface and \underline{n} is the unit outward normal vector and β is the Navier's wall slip coefficient, and is assumed to be dependent on the second invariant of the viscous stress tensor in the form:

$$\beta = \alpha \left(\frac{1}{2} (\underline{T} : \underline{T}) \right)^{(s_b - 1)/2} \quad (10)$$

The parameters of α and s_b are obtained from the rheological characterization of the material.

Constitutive Equation

The fluid is assumed to be a purely viscous generalized Newtonian fluid,

$$\underline{\tau} = -\eta(|\dot{\gamma}|) \dot{\underline{\gamma}} \quad (11)$$

where $\underline{\tau}$ is the viscous stress tensor, η is the shear viscosity function and $\dot{\underline{\gamma}}$ is the rate-of-deformation tensor.

The dependence of the shear viscosity material function η , on the deformation rate is assumed to follow the modified Herschel-Bulkley model (20) for viscoplastic fluids or its simplification the Ostwald-de Waele or Power Law model with $\tau_y = 0$:

$$\eta = \left[m(|\dot{\gamma}|)^{n-1} + \frac{\tau_y (1 - \exp(-n_b |\dot{\gamma}|))}{|\dot{\gamma}|} \right] \quad (12)$$

where n is the material parameter that governs the sensitivity of the fluid to deformation rate, τ_y is the yield stress, n_b is the stress growth exponent, and m is the consistency index. The magnitude of the rate of deformation tensor $|\dot{\gamma}|$ is defined for this case by:

$$|\dot{\gamma}|^2 = 2u_{r,r}^2 + 2\left(\frac{u_r}{r}\right)^2 + 2u_{z,z}^2 + (u_{r,z} + u_{z,r})^2 \quad (13)$$

where the comma indicates differentiation.

Determination of Force F

The z -component of the surface traction vector (assuming compressive stresses positive) is:

$$\pi = p + \tau_{zz} \quad (14)$$

and the total force needed to maintain the squeezing flow is obtained by integrating this traction over the surface of the top disk. Hence,

$$F = \int_0^R \int_0^{2\pi} ((p - p_a) + \tau_{zz})_{z=h} r dr d\theta \quad (15)$$

where p and τ_{∞} can be determined once u_r and u_z are obtained.

Numerical Solution

For the FEM solution of the momentum equations, the domain is discretized by the bilinear brick elements in r , and z , and trial functions are chosen such that:

$$u_r = \sum_{j=1}^{\text{Nod}} u_r^j \phi^j(r, z) \quad (16a)$$

$$u_z = \sum_{j=1}^{\text{Nod}} u_z^j \phi^j(r,z) \quad (16b)$$

$$u_r^j, u_z^j, \phi^j \in D^e \quad (16c)$$

where D^e is an element domain, Nod is the number of nodes per element, and $\phi^{\hat{z}}$ is the trial function. The weak form of the weighted residual equation is given below:

$$\int_{D^e} \left\{ 2\eta r \frac{\partial \phi^i}{\partial r} \frac{\partial u_r}{\partial r} + \eta r \frac{\partial \phi^i}{\partial z} \left(\frac{\partial u_r}{\partial z} + \frac{\partial u_z}{\partial r} \right) + 2\eta \phi^i \frac{u_r}{r} \right\} dr dz$$

$$+ \lambda_p \int_{D^e} \left(\eta r \frac{\partial \phi^i}{\partial r} + \eta \phi^i \right) \left(\frac{\partial u_r}{\partial r} + \frac{u_r}{r} + \frac{\partial u_z}{\partial z} \right) dr dz$$

$$+ \int n_r \phi^i (p + \tau_{rr}) r ds + \int n_z \phi^i \tau_{rz} r ds \quad (17a)$$

$$\int_{D^e} \left\{ 2\eta r \frac{\partial \phi^i}{\partial z} \frac{\partial u_z}{\partial z} + \eta r \frac{\partial \phi^i}{\partial r} \left(\frac{\partial u_r}{\partial z} + \frac{\partial u_z}{\partial r} \right) \right\} dr dz$$

$$+ \lambda_p \int_{D^e} \left(\eta r \frac{\partial \phi^i}{\partial z} \right) \left(\frac{\partial u_r}{\partial r} + \frac{u_r}{r} + \frac{\partial u_z}{\partial z} \right) dr dz$$

$$+ \int n_z \phi^i (p + \tau_{zz}) r ds + \int n_r \phi^i \tau_{rz} r ds \quad (17b)$$

where n_r and n_z are the components of the outward unit normal vector \underline{n} to the surface.

Results and Discussion

The major focus of the paper was the attempt to determine whether a one-dimensional lubrication approximation solution of the squeeze flow (18) is sufficient to represent the squeeze flow behavior of viscoplastic fluids subject to wall slip accurately. Thus, a series of comparisons between the results of one dimensional analytical solution and two-dimensional FEM based solutions were made for conditions which allowed the shear stress values to be significantly greater than the extensional stress terms in the equations of motion i.e., $h \ll R$. The comparisons will be made in terms of the velocity distributions and normal force values calculated with the two methods.

Table 1 contains the material parameters and the geometry and operating conditions used for the comparisons of the force values and the radial velocity distributions. The gap to the radius ratio (h/R) is kept at 0.048. The disk radius and the axial velocity of the disk are taken such that they can be

conveniently generated in the laboratory using a typical Instron Capillary tester. The comparisons of the force values predicted in 1-D and 2-D are shown in Table 2 for various values of the wall slip coefficient. Under the no slip condition and for relatively small values of the slip coefficient the 1-D solution (which does not include any extensional stress terms) agrees with the results of the 2-D FEM based solution (which incorporates the extensional stress terms). The 1-D solution however significantly underpredicts the force values as the wall slip coefficient increases. This is expected since the inclusion of wall slip should reduce the relative importance of the shear stress versus the extensional stress terms.

The comparisons of the force values predicted with the 1-D and 2-D analyses for various values of the yield stress are shown in Table 3. Under the moderate values of the yield stress which are used the predictions of the two methods agree well. Although these comparisons are encouraging for the use of the 1-D analytical models for the squeeze flow, it should be noted that there is no apriori method available to determine the conditions under which the assumptions of the 1-D model break down. Therefore, the analysis of the squeeze flow rheometer needs to be done by using a combination of both analytical and numerical techniques.

The same conclusions can be drawn by comparing the radial velocity distributions shown in Figures 1-2. For the power law fluid used to generate the results of Figure 2 the agreement between the velocity distributions determined with 1-D analysis with 2-D FEM solution is excellent. This is consistent with the findings of Zhang et al. (11) which have indicated that at relatively low squeeze rates and h/R values the lubrication assumption holds, and the elasticity of the polymer has a negligible contribution (low Deborah number case) since the generalized Newtonian fluid model is satisfactory to represent the rheological behavior of the melt.

The typical radial velocity distributions obtained with the viscoplastic fluid are shown in Figures 3-4 for the no-slip condition. The introduction of the viscoplasticity blunts the velocity distribution at any radial location. However, as dictated by the continuity equation the axial movement of the top plate generates a radial extensional flow where the radial velocity at the edge is the highest and the velocity decreases as one approaches the axis of symmetry. However, the fact that 1-D and 2-D solutions agree so well suggests that the magnitude of the shear stress is still significantly greater than the extensional stresses under these geometry and operating conditions, thus vindicating the validity of lubrication assumption for these conditions. However, as noted earlier the conditions under which the 1-D analysis are valid cannot be determined without the benefit of numerical analysis, as demonstrated here. The FEM based numerical analysis presented here should be

very useful in the analysis of the data generated with the squeeze flow rheometer and the determination of parameters of constitutive equations for the low Deborah number conditions for which the elasticity of the melt is not important.

References

1. Metzner, A. B., *J. Lubr. Techn.*, 90, 531 (1968).
2. Stefan, J., *Akad. Wiss. Math. Natur.*, Wien, 69, 713 (1974).
3. Scott, J. R., *Trans. Inst. Rubber Ind.*, 7, 169 (1931).
4. Leider P., *Ind. Eng. Chem. Fund.*, 13, 342 (1974).
5. Brindley G., J. Davies and K. Walters, *J. Non-Newtonian Fluid Mech.*, 1, 19 (1976).
6. Lee S., M. M. Denn, M. J. Crochet and A. B. Metzner, *J. Non-Newtonian Fluid Mech.*, 10, 3 (1982).
7. Chatraei S., C. W. Macosko and H. H. Winter, *J. Rheol.*, 25, 433 (1981).
8. Papanastasiou A. C., C. W. Macosko and L. E. Scriven, in "Interrelations between Processing Structure and Properties of Polymeric Materials", J. Seferis and P. Theocorsis, ed., Elsevier, Amsterdam (1984).
9. Tischny, J. and W. Winer, *J. Lubr. Techn.*, 100, 56 (1978).
10. Lee S., M. M. Denn, M. J. Crochet, A. B. Metzner and G. J. Riggins, *J. Non-Newtonian Fluid Mech.*, 14, 301 (1984).
11. Zhang, W., N. Silvi and J. Vlachopoulos, "Modelling and Experiments of Squeezing Flow of Polymeric Melts", *Intern. Polym. Proc.*, 10, 155 (1995).
12. Reynolds O., "On the Theory of Lubrication and its Application to Mr. Beauchamps Tower's Experiments", *Phil. Trans. Royal Soc.*, 177, 157 (1886).
13. Lipsomb G. G. and M. M. Denn, "Flow of Bingham Fluids in Complex Geometries", *J. Non-Newtonian Fluid Mech.*, 14, 337 (1984).
14. Wilson S. D., "Squeezing Flow of a Bingham Material", *J. Non-Newtonian Fluid Mech.*, 47, 211 (1993)
15. Yilmazer, U. and D. Kalyon., *J. Rheol.*, 37, 35 (1993).
16. Gartling D. K. and N. Phan-Thien, *J. Non-Newtonian Fluid Mech.*, 14, 347 (1984).
17. O'Donovan E. J. and R. J. Tanner, *J. Non-Newtonian Fluid Mech.*, 15, 75 (1984).
18. Lawal A. and D. M. Kalyon, "Squeezing Flow of Viscoplastic Fluids Subject to Wall Slip", accepted to appear in *Polym. Eng. Sci.* (1998).
19. Bird R. B., R. C. Armstrong and O. Hassager, "Dynamics of Polymeric Liquids", 2nd Ed., Volume 1, John Wiley & Sons (1997).
20. Papanastasiou, T. C., *J. Rheol.*, 31, 385 (1987)

Table 1: Material parameters and geometry

Material Parameters:

Shear rate sensitivity parameter, $n = 0.45$
 $m = 5066 \text{ Pa}\cdot\text{s}^{0.45}$

Disk geometry and operating conditions:

Gap, $h = 0.00137 \text{ m}$

Disk Radius, $R = 0.0286 \text{ m}$

Top disk speed = $2.12\text{E}-5 \text{ m/s}$

Table 2: Comparison of the Force values obtained with 1-D analysis with lubrication approximation and 2-D FEM for various slip coefficient $\beta^* = \beta(m/\dot{h})(\dot{h}/R)^n$ values.

β^*	Force, N (1-D) Lubrication approximation	Force, N (2-D) FEM
0	180.4	182.3
0.5	86.5	89.1
1.0	50.9	54.1
2.0	26.8	30.6
3.0	18.0	22.1
5.0	10.9	15.1
10.0	5.4	9.8

Table 3: Comparison of force values obtained with 1-D analysis with lubrication approximation and 2-D FEM for various yield stress, $\tau_y^* = \tau_y/(m/(-\dot{h}/R)^n)$, values

τ_y^*	Force, N (1-D) Lubrication approximation	Force, N (2-D) FEM
0	180.4	182.3
25	395	408.2
50	596	623.3
75	791	833.3
100	982.3	1040.4

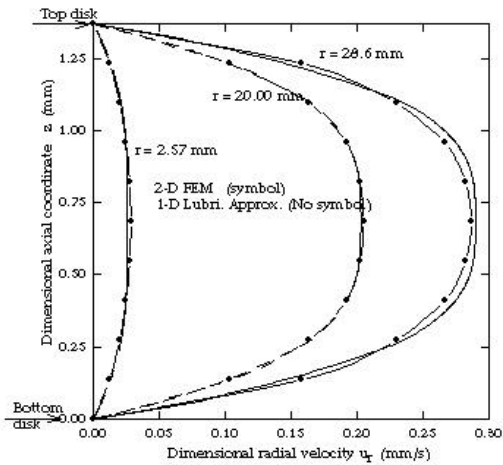


Fig. 1 Dimensional radial velocity profiles for the squeezing flow of a power law fluid without wall slip; $n = 0.45$, $\beta^* = 0.0$ and $h/R = 0.048$.

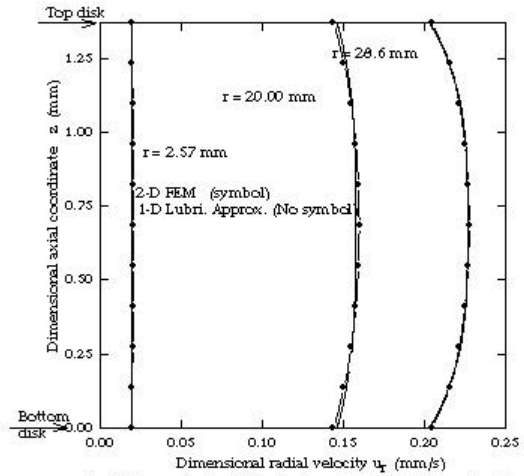


Fig. 2 Dimensional radial velocity profiles for the squeezing flow of a power law fluid with wall slip; $n = 0.45$, $\beta^* = 1.0$ and $h/R = 0.048$.

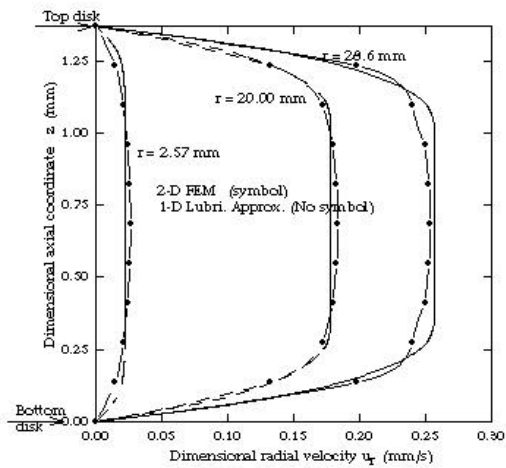


Fig. 3 Dimensional radial velocity profiles for the squeezing flow of a viscoplastic fluid without wall slip; $n = 0.45$, $\tau_y^* = 2.5$ and $h/R = 0.048$.

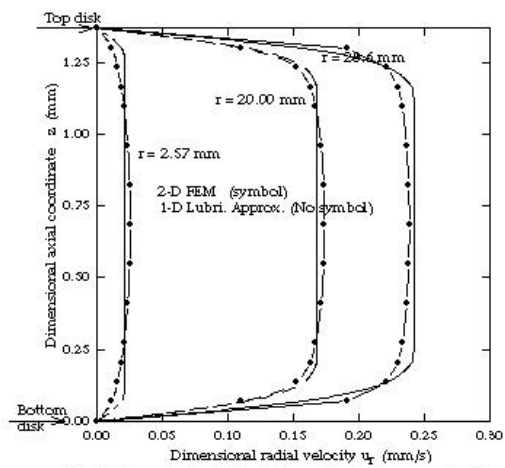


Fig. 4 Dimensional radial velocity profiles for the squeezing flow of a viscoplastic fluid without wall slip; $n = 0.45$, $\tau_y^* = 7.5$ and $h/R = 0.048$.